

# Semi-analytical approaches to gravitational radiation from astrophysical sources

José Fernando Rodríguez Ruiz

Universidad Industrial de Santander  
UIS, Bucaramanga, Colombia

# Adiabatic inspiral and heuristic view of the plunge<sup>1</sup>

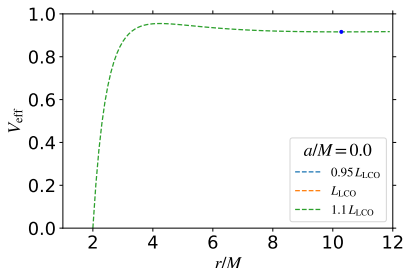
- ▶ Geometrized units and Boyer-Linquist coordinates  $(t, r, \theta, \phi)$ .
- ▶ Effective potential,  $m \equiv$  TP mass,  $M \equiv$  BH mass,  $a = S/M$ ,

$$V_{\text{eff}} = 1 - \frac{2M}{r} + \frac{[L^2/m^2 - a^2(E^2/m^2 - 1)]}{r^2} - \frac{2M(L/m - aE/m)^2}{r^3}$$

- ▶ Particle initially at a circular orbit

$$E_{\text{circ}}/m = (r^2 - 2Mr + aM^{1/2}r^{1/2})/[r(r^2 - 3Mr + 2aM^{1/2}r^{1/2})]^{1/2}$$

- ▶ Test particle falls due to GW radiation: sequence of circular orbits.
- ▶ Slow energy-angular momentum losses: adiabatic equation,  $\dot{r} = -\dot{E}_{\text{GW}}/(dE_{\text{circ}}/dr)$ ,  $dE_{\text{circ}}/dr|_{\text{LCO}} = 0$ . At LCO,  $E_{\text{circ}}$  reaches a minimum:  $\dot{r}|_{\text{LCO}} \rightarrow \infty$ : **PROBLEMS AT LCO!**



<sup>1</sup>Rodriguez, Rueda & Ruffini, *Astronomy Reports*, 62, 940

# Adiabatic inspiral and heuristic view of the plunge<sup>1</sup>

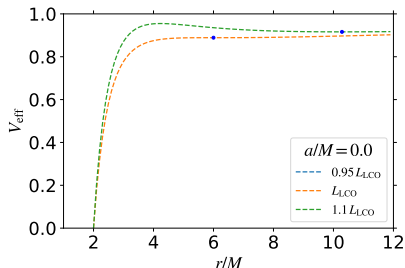
- ▶ Geometrized units and Boyer-Linquist coordinates  $(t, r, \theta, \phi)$ .
- ▶ Effective potential,  $m \equiv$  TP mass,  $M \equiv$  BH mass,  $a = S/M$ ,

$$V_{\text{eff}} = 1 - \frac{2M}{r} + \frac{[L^2/m^2 - a^2(E^2/m^2 - 1)]}{r^2} - \frac{2M(L/m - aE/m)^2}{r^3}$$

- ▶ Particle initially at a circular orbit

$$E_{\text{circ}}/m = (r^2 - 2Mr + aM^{1/2}r^{1/2})/[r(r^2 - 3Mr + 2aM^{1/2}r^{1/2})]^{1/2}$$

- ▶ Test particle falls due to GW radiation: sequence of circular orbits.
- ▶ Slow energy-angular momentum losses: adiabatic equation,  $\dot{r} = -\dot{E}_{\text{GW}}/(dE_{\text{circ}}/dr)$ ,  $dE_{\text{circ}}/dr|_{\text{LCO}} = 0$ . At LCO,  $E_{\text{circ}}$  reaches a minimum:  $\dot{r}|_{\text{LCO}} \rightarrow \infty$ : **PROBLEMS AT LCO!**



<sup>1</sup>Rodriguez, Rueda & Ruffini, *Astronomy Reports*, 62, 940

# Adiabatic inspiral and heuristic view of the plunge<sup>1</sup>

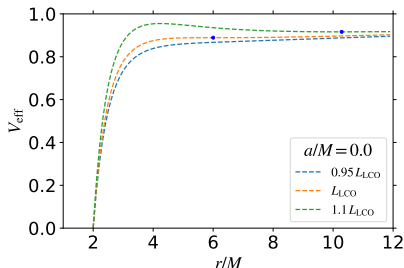
- ▶ Geometrized units and Boyer-Linquist coordinates  $(t, r, \theta, \phi)$ .
- ▶ Effective potential,  $m \equiv$  TP mass,  $M \equiv$  BH mass,  $a = S/M$ ,

$$V_{\text{eff}} = 1 - \frac{2M}{r} + \frac{[L^2/m^2 - a^2(E^2/m^2 - 1)]}{r^2} - \frac{2M(L/m - aE/m)^2}{r^3}$$

- ▶ Particle initially at a circular orbit

$$E_{\text{circ}}/m = (r^2 - 2Mr + aM^{1/2}r^{1/2})/[r(r^2 - 3Mr + 2aM^{1/2}r^{1/2})]^{1/2}$$

- ▶ Test particle falls due to GW radiation: sequence of circular orbits.
- ▶ Slow energy-angular momentum losses: adiabatic equation,  $\dot{r} = -\dot{E}_{\text{GW}}/(dE_{\text{circ}}/dr)$ ,  $dE_{\text{circ}}/dr|_{\text{LCO}} = 0$ . At LCO,  $E_{\text{circ}}$  reaches a minimum:  $\dot{r}|_{\text{LCO}} \rightarrow \infty$ : **PROBLEMS AT LCO!**



<sup>1</sup>Rodriguez, Rueda & Ruffini, *Astronomy Reports*, 62, 940

# Adiabatic inspiral and heuristic view of the plunge<sup>1</sup>

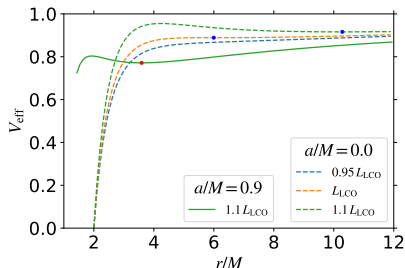
- ▶ Geometrized units and Boyer-Linquist coordinates  $(t, r, \theta, \phi)$ .
- ▶ Effective potential,  $m \equiv$  TP mass,  $M \equiv$  BH mass,  $a = S/M$ ,

$$V_{\text{eff}} = 1 - \frac{2M}{r} + \frac{[L^2/m^2 - a^2(E^2/m^2 - 1)]}{r^2} - \frac{2M(L/m - aE/m)^2}{r^3}$$

- ▶ Particle initially at a circular orbit

$$E_{\text{circ}}/m = (r^2 - 2Mr + aM^{1/2}r^{1/2})/[r(r^2 - 3Mr + 2aM^{1/2}r^{1/2})]^{1/2}$$

- ▶ Test particle falls due to GW radiation: sequence of circular orbits.
- ▶ Slow energy-angular momentum losses: adiabatic equation,  $\dot{r} = -\dot{E}_{\text{GW}}/(dE_{\text{circ}}/dr)$ ,  $dE_{\text{circ}}/dr|_{\text{LCO}} = 0$ . At LCO,  $E_{\text{circ}}$  reaches a minimum:  $\dot{r}|_{\text{LCO}} \rightarrow \infty$ : **PROBLEMS AT LCO!**



<sup>1</sup>Rodriguez, Rueda & Ruffini, *Astronomy Reports*, 62, 940

# Adiabatic inspiral and heuristic view of the plunge<sup>1</sup>

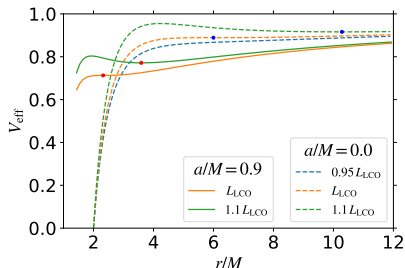
- ▶ Geometrized units and Boyer-Linquist coordinates  $(t, r, \theta, \phi)$ .
- ▶ Effective potential,  $m \equiv$  TP mass,  $M \equiv$  BH mass,  $a = S/M$ ,

$$V_{\text{eff}} = 1 - \frac{2M}{r} + \frac{[L^2/m^2 - a^2(E^2/m^2 - 1)]}{r^2} - \frac{2M(L/m - aE/m)^2}{r^3}$$

- ▶ Particle initially at a circular orbit

$$E_{\text{circ}}/m = (r^2 - 2Mr + aM^{1/2}r^{1/2})/[r(r^2 - 3Mr + 2aM^{1/2}r^{1/2})]^{1/2}$$

- ▶ Test particle falls due to GW radiation: sequence of circular orbits.
- ▶ Slow energy-angular momentum losses: adiabatic equation,  $\dot{r} = -\dot{E}_{\text{GW}}/(dE_{\text{circ}}/dr)$ ,  $dE_{\text{circ}}/dr|_{\text{LCO}} = 0$ . At LCO,  $E_{\text{circ}}$  reaches a minimum:  $\dot{r}|_{\text{LCO}} \rightarrow \infty$ : **PROBLEMS AT LCO!**



<sup>1</sup>Rodriguez, Rueda & Ruffini, *Astronomy Reports*, 62, 940

# Adiabatic inspiral and heuristic view of the plunge<sup>1</sup>

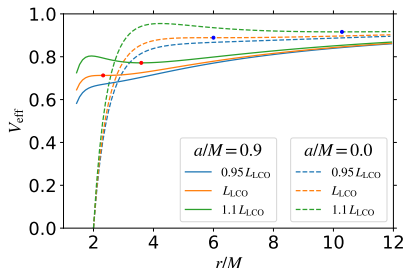
- ▶ Geometrized units and Boyer-Linquist coordinates  $(t, r, \theta, \phi)$ .
- ▶ Effective potential,  $m \equiv$  TP mass,  $M \equiv$  BH mass,  $a = S/M$ ,

$$V_{\text{eff}} = 1 - \frac{2M}{r} + \frac{[L^2/m^2 - a^2(E^2/m^2 - 1)]}{r^2} - \frac{2M(L/m - aE/m)^2}{r^3}$$

- ▶ Particle initially at a circular orbit

$$E_{\text{circ}}/m = (r^2 - 2Mr + aM^{1/2}r^{1/2})/[r(r^2 - 3Mr + 2aM^{1/2}r^{1/2})]^{1/2}$$

- ▶ Test particle falls due to GW radiation: sequence of circular orbits.
- ▶ Slow energy-angular momentum losses: adiabatic equation,  $\dot{r} = -\dot{E}_{\text{GW}}/(dE_{\text{circ}}/dr)$ ,  $dE_{\text{circ}}/dr|_{\text{LCO}} = 0$ . At LCO,  $E_{\text{circ}}$  reaches a minimum:  $\dot{r}|_{\text{LCO}} \rightarrow \infty$ : **PROBLEMS AT LCO!**



<sup>1</sup>Rodriguez, Rueda & Ruffini, *Astronomy Reports*, 62, 940

## Hamiltonian approach and helicoidal drifting sequence (HDS)<sup>2</sup>

- ▶ The Hamiltonian of the test particle of mass  $m$  in the field of the Kerr black hole of mass  $M$  is given by

$$H = -p_t = -N^i p_i + N \sqrt{m^2 + \gamma^{ij} p_i p_j}, \quad (1)$$

where  $N = 1/\sqrt{-g^{00}}$ ,  $N^i = -g^{ti}/g^{tt}$ ,  $\gamma^{ij} = g^{ij} - g^{ti}g^{tj}/g^{tt}$ .

- ▶ Dynamical equations are:

$$\dot{r} = \frac{\partial H}{\partial p_r} \qquad \Omega \equiv \dot{\phi} = \frac{\partial H}{\partial L}, \quad (2)$$

$$\dot{p}_r = -\frac{\partial H}{\partial r} + \mathcal{F}_r^{\text{nc}} \qquad \dot{p}_\phi = -\mathcal{F}_\phi^{\text{nc}} \quad (3)$$

where  $\mathcal{F}_r^{\text{nc}}$  and  $\mathcal{F}_\phi^{\text{nc}}$  are the radial and azimuthal non-conservative radiation-reaction forces.

---

<sup>2</sup>Rodriguez, Rueda & Ruffini, *Astronomy Reports*, 62, 940



## Hamiltonian approach and helicoidal drifting sequence (HDS)<sup>2</sup>

- ▶ The Hamiltonian of the test particle of mass  $m$  in the field of the Kerr black hole of mass  $M$  is given by

$$H = -p_t = -N^i p_i + N \sqrt{m^2 + \gamma^{ij} p_i p_j}, \quad (1)$$

where  $N = 1/\sqrt{-g^{00}}$ ,  $N^i = -g^{ti}/g^{tt}$ ,  $\gamma^{ij} = g^{ij} - g^{ti}g^{tj}/g^{tt}$ .

- ▶ Dynamical equations are: **Circular orbits**

$$\dot{r} = \frac{\partial H}{\partial p_r} = 0 \quad \Omega \equiv \dot{\phi} = \frac{\partial H}{\partial L}, \quad (2)$$

$$\dot{p}_r = -\frac{\partial H}{\partial r} = 0 \quad \dot{p}_\phi = 0 \quad (3)$$

where  $\mathcal{F}_r^{\text{nc}}$  and  $\mathcal{F}_\phi^{\text{nc}}$  are the radial and azimuthal non-conservative radiation-reaction forces.

- ▶ Particle falls due to the loss of energy and angular momentum, and explicit contribution of the conservative radial force.

---

<sup>2</sup>Rodriguez, Rueda & Ruffini, **Astronomy Reports**, 62, 940

## Hamiltonian approach and helicoidal drifting sequence (HDS)<sup>2</sup>

- ▶ The Hamiltonian of the test particle of mass  $m$  in the field of the Kerr black hole of mass  $M$  is given by

$$H = -p_t = -N^i p_i + N \sqrt{m^2 + \gamma^{ij} p_i p_j}, \quad (1)$$

where  $N = 1/\sqrt{-g^{00}}$ ,  $N^i = -g^{ti}/g^{tt}$ ,  $\gamma^{ij} = g^{ij} - g^{ti}g^{tj}/g^{tt}$ .

- ▶ Dynamical equations are:

$$\dot{r} = \frac{\partial H}{\partial p_r} \qquad \Omega \equiv \dot{\phi} = \frac{\partial H}{\partial L}, \quad (2)$$

$$\dot{p}_r = -\frac{\partial H}{\partial r} + \mathcal{F}_r^{\text{nc}} \qquad \dot{p}_\phi = -\mathcal{F}_\phi^{\text{nc}} \quad (3)$$

where  $\mathcal{F}_r^{\text{nc}}$  and  $\mathcal{F}_\phi^{\text{nc}}$  are the radial and azimuthal non-conservative radiation-reaction forces.

- ▶ Particle falls due to the loss of energy and angular momentum, and explicit contribution of the conservative radial force.
- ▶ Adiabatic parameter  $\eta \equiv \dot{\Omega}/\Omega^2 \approx \dot{r}/(r\Omega) \ll 1$ .
- ▶ All dynamical variables are finite at LCO

---

<sup>2</sup>Rodriguez, Rueda & Ruffini, *Astronomy Reports*, 62, 940

## How to calculate $\dot{E}_{\text{GW}}$ and $\dot{L}_{\text{GW}}$ ? GWR from circular Orbits on Kerr Spacetime

- ▶ Test particle in a stable circular orbit at  $r$  and co-rotating with the BH

$$\Omega_{\text{corot}} = \frac{M^{1/2}}{(r^{3/2} + aM^{1/2})} \quad (4)$$

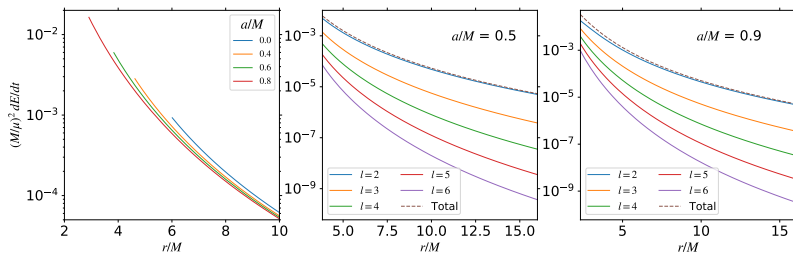
- ▶ The energy and angular momentum fluxes to  $\infty$  are given in terms of  $Z_{lm\omega}^H$ , which are obtained from BH perturbation theory [Teukolsky, **ApJ**, 185, 635 (1973)], namely by solving the Sasaki-Nakamura Eq. [Sasaki & Nakamura, **Phys. Lett. A**, 86, 68 (1982)]:

$$\frac{dE}{dt} = \sum_{l,m} \frac{\infty}{4\pi\omega_m^2} |\tilde{Z}_{lm\omega}^H|^2, \quad (5)$$

$$\frac{dL}{dt} = \sum_{l,m} \frac{\infty}{4\pi\omega_m^3} m|\tilde{Z}_{lm\omega}^H|^2, \quad (6)$$

- ▶ The GW angular frequency for each multipole  $\omega_m = m\Omega$
- ▶ **NO RADIATION FROM CIRCULAR ORBITS INSIDE THE LCO.**

# Energy Flux



Energy fluxes to infinite test particle in a circular orbit. Rodriguez, Rueda & Ruffini, **Astronomy Reports**, 62, 940

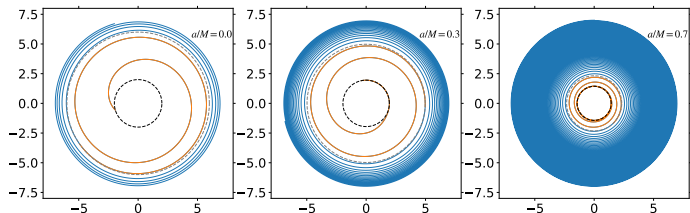
- For quasi-circular, adiabatic motion we have:

$$\mathcal{F}_r^{\text{nc}} = 0, \quad (7)$$

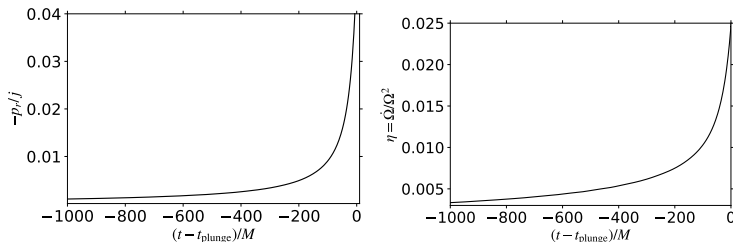
$$\mathcal{F}_\phi^{\text{nc}} = -\frac{1}{\Omega} \frac{dE}{dt}. \quad (8)$$

## Test particle dynamics in HDS approach

- ▶ Test particle trajectories  $\nu = mM/(m + M)^2 = 0.01$ , for different  $a/M$ :



- ▶ The dynamics includes the contribution of the radial momentum which is not negligible near the LCO.
- ▶  $t_{\text{plunge}}$  is defined as the time when the particle crosses the LCO in the HDS.



Left: ratio  $-p_r/(p_\phi/m) = p_r/j$  for  $a/M = 0.9$ . Right: Adiabatic parameter. Rodriguez, Rueda, & Ruffini, Astronomy Reports, 62, 940 (2018)

## Transition to plunge: comparison with other approaches

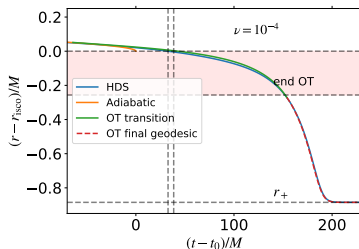
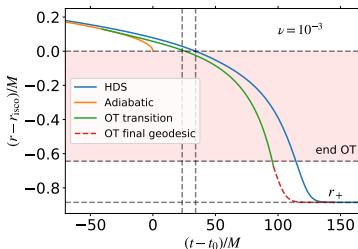
- ▶ Taylor expansion of  $V_{\text{eff}}$  around the LCO<sup>3</sup>:

$$\ddot{r} = \partial_r^3 F|_{\text{LCO}}(r - r_{\text{LCO}})^2/4 + \partial_r E F|_{\text{LCO}}(E - E_{\text{LCO}}^{\text{circ}})/2 + \partial_r L F|_{\text{LCO}}(L - L_{\text{LCO}}^{\text{circ}})/2,$$

where,  $F := r^4 \frac{V_{\text{eff}}}{V_t^2}$ ,  $V_t = \frac{aL}{m} + \frac{r^2 + a^2}{m(r^2 - 2Mr + a^2)} [E(r^2 + a^2) - La]$

- ▶ Energy and angular momentum losses evaluated at LCO ( $r_{\text{adiab}}(t_0) = r_{\text{LCO}}$ ,  $t_0 \neq t_{\text{plunge}}$ )

$$(E - E_{\text{LCO}}^{\text{circ}}) = (t - t_0) \dot{E}_{\text{GW}}|_{\text{LCO}}, \quad (L - L_{\text{LCO}}^{\text{circ}}) = (t - t_0) \Omega^{-1} \dot{E}_{\text{GW}}|_{\text{LCO}}.$$



Comparison  $a/M = 0.9$ . See Rodriguez, J. F., Rueda, J. A., and Ruffini, R, Astr. Rep., 2018, 62, 940

- ▶ **GW radiation at the same rate as the LCO, long after the test particle has passed it.**

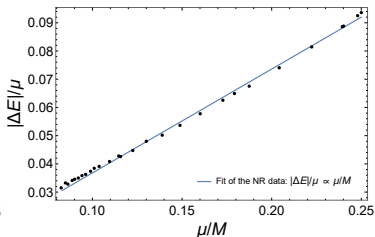
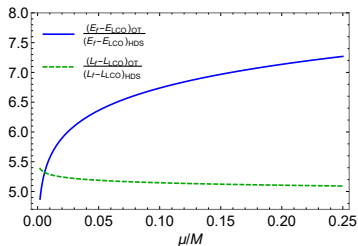
<sup>3</sup>Ori & Thorne, *Phys. Rev. D*, 62, 124022 (2000); Sundararajan, *Phys. Rev. D*, 77, 124050 (2008)

## Comparison with other works

- ▶ The energy “deficits” at the end:

$$\Delta E_{\text{def}} = E_{\text{LCO}}^{\text{circ}} - E_{\text{plunge,f}}^{\text{formalism}} \quad (9)$$

- ▶  $E_{\text{plunge,f}}^{\text{HDS}} := H(t_{\text{plunge}}) < E_{\text{LCO}}^{\text{circ}}$



Our work: Rodriguez, J. F., Rueda, J. A., and Ruffini, R, Astronomy Reports, 2018, Vol. 62, No. 12, pp. 940–952. Comparison with Ori & Thorne (2000) (left) and NR from SXS catalog <https://www.black-holes.org/> (right)

- ▶ In the HDS there is less radiated energy (angular momentum) than in the results of Ori & Thorne (2000).

## Semi-analytic approach to binary black holes (comparable masses)

- ▶ Motivation: work of Aninos et al. (1995) (among other works), also as a “working hypothesis”  $\leadsto$  Newtonian center-of-mass point of view



# Semi-analytic approach to binary black holes (comparable masses)

- ▶ Motivation: work of Aninos et al. (1995) (among other works), also as a “working hypothesis”  $\leadsto$  Newtonian center-of-mass point of view

## Principles of “test particle waveform” formalism

1. Test particle orbits on **Kerr spacetime**: **HDS approach**
2. GW emission back-reaction given by circular orbits up to LCO
3. Plunge geodesic

# Semi-analytic approach to binary black holes (comparable masses)

- ▶ Motivation: work of Aninos et al. (1995) (among other works), also as a “working hypothesis”  $\leadsto$  Newtonian center-of-mass point of view

## Principles of “test particle waveform” formalism

1. Test particle orbits on **Kerr spacetime**: **HDS approach**
2. GW emission back-reaction given by circular orbits up to LCO
3. Plunge geodesic
4. From test particle to comparable masses  $m_1/m_2 \approx 1$ :  $m_{\text{test}} \mapsto \mu$ ,  $M \mapsto m_{\text{tot}} = m_1 + m_2$

# Semi-analytic approach to binary black holes (comparable masses)

- ▶ Motivation: work of Aninos et al. (1995) (among other works), also as a “working hypothesis”  $\leadsto$  Newtonian center-of-mass point of view

## Principles of “test particle waveform” formalism

1. Test particle orbits on **Kerr spacetime**: **HDS approach**
2. GW emission back-reaction given by circular orbits up to LCO
3. Plunge geodesic
4. From test particle to comparable masses  $m_1/m_2 \approx 1$ :  $m_{\text{test}} \mapsto \mu$ ,  $M \mapsto m_{\text{tot}} = m_1 + m_2$

## “Test particle” waveform construction

1. The gravitational waveform can be constructed from “circularized waves”:

$$\frac{1}{2} (h_+ - ih_\times) = -\frac{1}{R} \sum_{l,m} \frac{Z_{lm\omega}^H}{\omega_m^2} {}_{-2}S_{lm}(\Theta) e^{im\Phi} e^{-i\omega_m(t-R^*)}, \quad (10)$$

where  $R$  is the distance to the observer,  $\Theta$  is the angle between the axis of rotation and the observer,  $\Phi$  is the azimuthal coordinate of the orbiting body at  $t = 0$ ;  $R^*$  is the Kerr “tortoise”.

2. The complex number  $Z_{lm\omega}$  evolves with time, inducing a variable wave amplitude and phase shift.

$(r(t), \phi(t))$  “test particle” trajectory coordinates

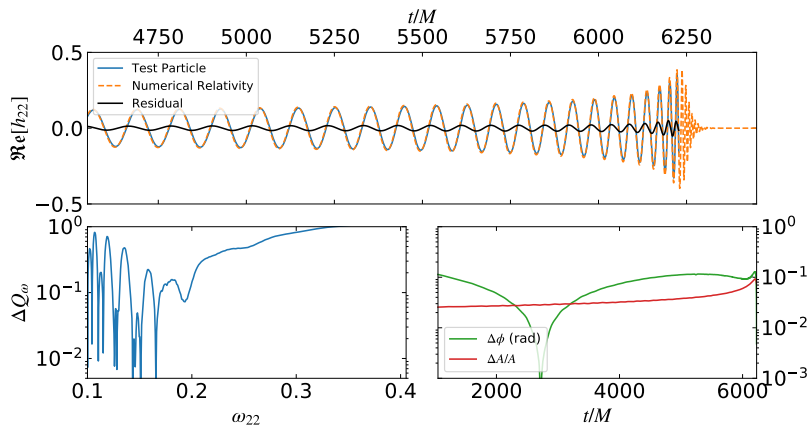
$$\omega_m(t - R^*) \mapsto m\phi(t - R^*).$$

# “Test particle” and NR waveforms

Intrinsic phase-time parameter  $Q_\omega = \omega^2 / \dot{\omega}$

## Working hypothesis

HDS + Newtonian center-of-mass



Numerical-relativity waveform BBH:0230,  $m_1 = m_2$  and initial spins  $a_1/m_1 = a_2/m_2 = 0.8$ , final Kerr BH spin  $a_f/M_f = 0.907516$ . Intrinsic time-domain phase difference evolution  $\Delta Q_\omega = |Q_\omega^{\text{TP}} - Q_\omega^{\text{NR}}|$

## Comparison with NR

- ▶ BBH numerical relativity simulations with equal masses components,  $m_1/m_2 = q$ . Initial components can have equally aligned spins  $a_1/m_1 = a_2/m_2$ . We studied the special case without spin (two Schwarzschild BHs).
- ▶ Fitting factor F,

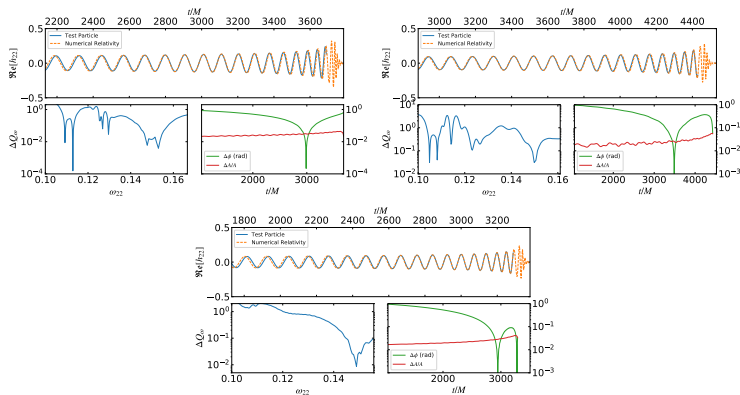
$$F \equiv (h_1|h_2)/\sqrt{(h_1|h_1)(h_2|h_2)}, \quad (h_1|h_2) \equiv 4\Re\left[\int_0^\infty h_1(f)\tilde{h}_2(f)/S_n(f)df\right],$$

Simulation	$a_i/m_i$	$a_f/M_f$	$a_{\text{eff}}/M_f$	F
BBH:0001	$1.209309 \times 10^{-7}$	0.686461	0.36	0.96
BBH:0157	0.949586	0.940851	0.99	0.93
BBH:0228	0.600000	0.857813	0.80	0.972
BBH:0230	0.800000	0.907516	0.9075	0.993

Rodriguez, J. F., Rueda, J. A. and Ruffini, R, **JCAP**, 2018, 030

# Spin-less merging components

- ▶ BBH simulations with spin-less initial components and different mass ratios  $q < 1$



SXS spinless BBH simulations <https://www.black-holes.org/>, BBH:0169,  
 $q = 1/2$ ,  $a_{\text{eff}} = 0.33$ ; BBH:0169,  $q = 1/3$ ,  $a_{\text{eff}} = 0.329$ ; BBH:0169,  $q = 1/4$ ,  $a_{\text{eff}} = 0.25$ .  
Rodriguez, J. F., Rueda, J. A. and Ruffini, R, **JCAP**, 2018, 030

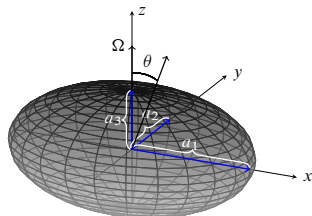
“FRAME DRAGGING” DUE TO THE ORBITAL ANGULAR MOMENTUM

## Incompressible ellipsoidal figures of equilibrium

- ▶ Classical work of Chandrashekar, *Ellipsoidal Figures of Equilibrium* (1969)
- ▶ Evolution of incompressible self-gravitating object driven by GW reaction  $\implies$  conserved quantity: circulation along the equator. Bonnie, D. Miller, *The Astrophysical Journal*, 187, 606, (1974).
- ▶ Evolution along Riemann S-type (self-gravitating object supported by rotation and internal motions) sequence with constant circulation  $C$ ,

$$C = \pi a_1 a_2 (\zeta + 2\Omega),$$

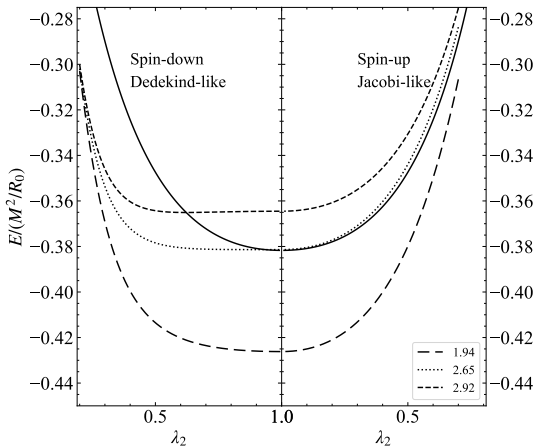
where  $\Omega$  spin and  $\zeta$  vorticity, and they are parallel.



A compressible ellipsoid characterized by the polytropic index  $n$ ,  $\lambda_2 := a_2/a_1$ ,  $\lambda_3 := a_3/a_1$ ,  $\Omega$  and vorticity  $\zeta$

## Compressible models: polytropic EOS

- ▶ Generalization to objects whose internal matter is described by a polytropic EOS [Lai, Rasio & Shapiro, **ApJ** **S**, 88, 205 (1993)].
- ▶ Time unit  $\tau_{\text{CEL}} = (\pi G \bar{\rho}_0)^{-1/2}$ , where  $\bar{\rho}_0 = M/(4/3\pi R_0^3)$ ,  $R_0 :=$  radius of the non-rotating polytrope (same  $n$ ) with the same mass.
- ▶ Evolution *a la* Landau-Lifshitz

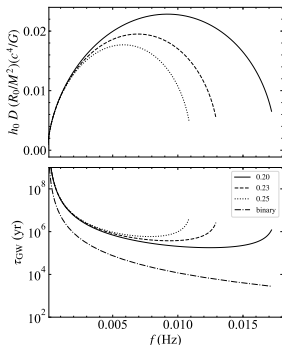


Quasi-static evolution of a CEL with  $n = 1$  and different circulations  $C/\pi = 1.95, 2.39, 2.92$



## Polytropic index $n \rightarrow 3$ : chirping ellipsoid (CEL)

- ▶ **New phenomena:** Early period increasing GW frequency and amplitude
- ▶ typical frequency is  $\sim 1$  mHz. Space-based interferometers: LISA, TianQin.



GW strain and timescale of a CEL with  $n = 2.95$ ,  $M = 1.0 M_\odot$  which is the same of the non-rotating spherical star with radius  $R \approx 6000$  km. The value of the circulation for the continuous, dashed and dotted line are  $\mathcal{C} = (\kappa_n MC/5\pi)/(GM^3 R_0)^{1/2} = (0.20, 0.23, 0.25)$ , respectively. Rodriguez, Rueda, Ruffini, Zuluaga, Iglesias-Blanco and Loren-Aguilar, JCAP 2023.

## Intrinsic GW phase-time evolution of CELs

- ▶ CELs are quasi-monochromatic
- ▶ Intrinsic phase-time parameter  $Q_\omega \equiv \frac{\omega^2}{\dot{\omega}} = \frac{d\phi}{d \ln \omega} = 2\pi \frac{dN}{d \ln f}$

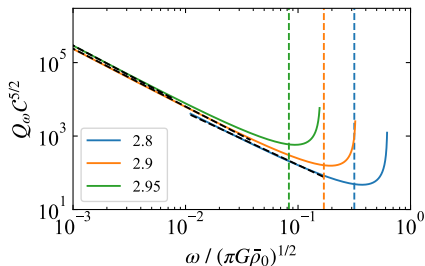


Figure 1: Intrinsic phase-time of CELs with  $n = 2.8, 2.9, 2.95$ . Rodriguez, Rueda, Ruffini, Zuluaga, Iglesias-Blanco and Loren-Aguilar, **JCAP 2023**.

- ▶ Intrinsic phase empirical fits,

$$Q_\omega^{\text{CEL}} \approx \frac{A_n}{C^{5/2}} \left[ \frac{\omega}{\sqrt{\pi G \bar{\rho}_0}} \right]^\alpha \quad C = GM_{\text{CEL}} / (c^2 R_0)$$

- ▶ Intrinsic phase-time evolution of Newtonian binaries

$$Q_\omega^{\text{bin}} = \frac{5}{3} 2^{-7/3} (\omega M_{\text{chirp}})^{-5/3}$$

- ▶ Polytropic structure constants ( $n, \kappa_n, k_1, k_2, k_3$ ) and the  $Q_\omega$  power-law empirical fitting parameters.

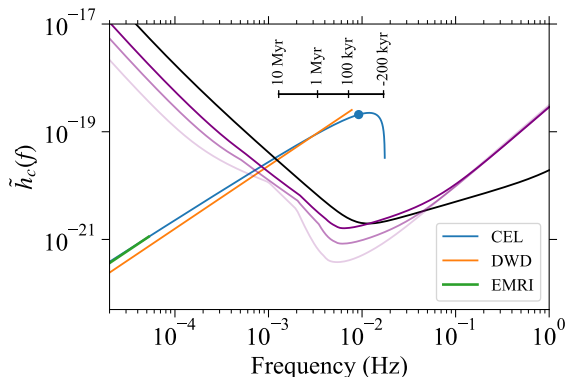
$n$	$\kappa_n$	$k_1$	$k_2$	$k_3$	$\mathcal{A}_n$	$\alpha$
1.0	0.65345	0.5	0.81289	2.2472	2.68	-1.081
2.0	0.38712	1.1078	0.71618	1.6562	4.003	-1.222
2.5	0.27951	1.4295	0.67623	1.4202	4.060	-1.447
2.7	0.24109	1.55971	0.66110	1.33194	5.926	-1.365
2.9	0.20530	1.69038	0.64630	1.24621	4.940	-1.571
2.95	0.19676	1.72309	0.64265	1.22511	4.369	-1.614
2.97	0.19340	1.73617	0.64119	1.21669	3.760	-1.640
2.99	0.19005	1.74925	0.63973	1.20829	3.817	-1.652

- ▶ In the limit  $n \rightarrow 3, \alpha \rightarrow -5/3$ : CEL-binary equivalence,

$$Q_\omega^{\text{CEL}} = Q_\omega^{\text{bin}} \iff \frac{M_{\text{CEL}}}{M_{\text{chirp}}} = 2^{7/5} \left( \frac{3A_3}{5} \right)^{3/5} \sqrt{3/4}$$

## CELS detection

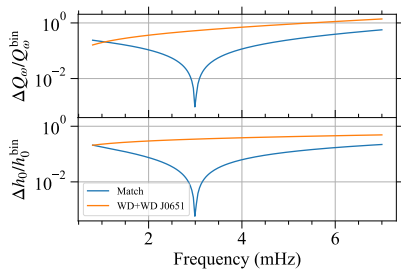
$$\tilde{h}_c(f) = h_0(f)\sqrt{N} = h_0(f)\sqrt{fT_{\text{obs}}},$$



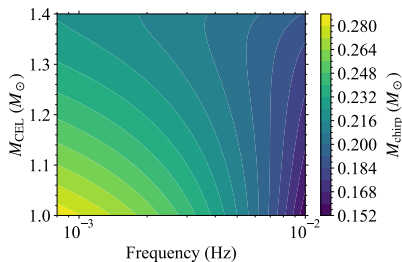
Reduced characteristic amplitude,  $\tilde{h}_c$ , of a CEL, a double WD (DWD) and an EMRI. The CEL has a mass  $M_{\text{CEL}} = 1.0 M_{\odot}$  and compactness  $C \approx 2.5 \times 10^{-4}$  (blue), according to the relativistic Feynman-Metropolis-Teller EOS. The polytropic index is  $n = 2.95$ , and is located at a distance  $D = 1$  kpc. The observing time has been set to  $T_{\text{obs}} = 2$  yr.. Rodriguez, Rueda, Ruffini, Zuluaga, Iglesias-Blanco and Loren-Aguilar, JCAP 2023

# CEL-binary degeneration

Rodriguez, Rueda, Ruffini, Zuluaga, Iglesias-Blanco and Loren-Aguilar, JCAP 2023



CEL ( $n = 2.95$ ) with  $M_{\text{CEL}} = 1.0 M_{\odot}$  and  $C = 2.5 \times 10^{-4}$ , and an equivalent binary system with  $M_{\text{bin}} = 0.24 M_{\odot}$ . Also comparison of the CEL signal with that of the detached binary DWD J0651 ( $M_{\text{chirp}} = 0.31 M_{\odot}$ ).



Contours of constant chirp mass of the equivalent binary as a function of the CEL mass and the observed frequency. In general, the chirp mass of the equivalent binary depends on the  $C$ ,  $M_{\text{CEL}}$ , and on the observed frequency  $f$ . However, once the EOS is selected, the mass-radius relation is fixed implying that  $M_{\text{chirp}}$  depends only on  $M_{\text{CEL}}$  and  $f$ .

## CEL-binary degeneration

- Phase difference during 1 yr,

$$\Delta\phi_{1y} = \int_{\omega_0}^{\omega_{1yr}} \Delta Q_{\omega} d \ln \omega,$$

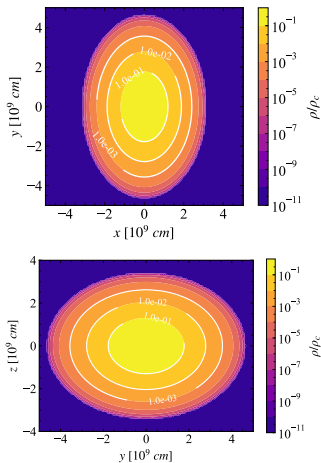
where  $\Delta Q_{\omega} = |Q_{\omega}^{\text{CEL}} - Q_{\omega}^{\text{bin}}|$

- End for EMRIs:  $f_{\text{td}} \approx (Gm_2/R_2^3)^{1/2}/(2.4^{3/2}\pi)$ ,
- End for DWD: frequency when one of the components fills its Roche-lobe.
- CEL-binary equivalence parameters, Rodriguez, Rueda, Ruffini, Zuluaga, Iglesias-Blanco and Loren-Aguilar, JCAP 2023

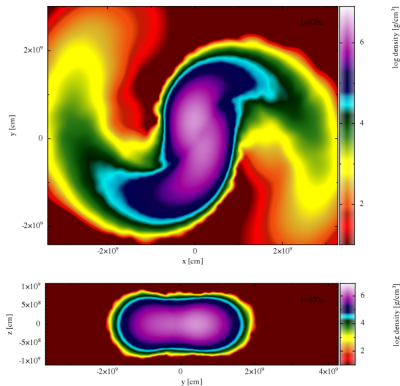
$M_{\text{CEL}}$ ( $M_{\odot}$ )	$C$ ( $10^{-4}$ )	$f_{\text{end}}^{\text{CEL}}$ (mHz)	$M_{\text{chirp}}$ ( $M_{\odot}$ )	$m_1$ ( $M_{\odot}$ )	$m_2$ ( $M_{\odot}$ )	$f_{\text{end}}^{\text{bin}}$ (mHz)	Type-like	$f_0$ (mHz)	$\Delta\phi_{1y}$	$\frac{\Delta h_0}{h_0}  _{1y}$	$\frac{D_{\text{CEL}}}{D_{\text{bin}}}$	SNR
1.0	2.5	9.20	0.32	1940.62	0.0001	0.053	EMRI	0.05	$3.631 \times 10^{-10}$	$5.937 \times 10^{-13}$	0.778	und.
			0.28	0.35	0.30	13.38	PG1101+364	1.0	$5.004 \times 10^{-5}$	$2.515 \times 10^{-9}$	0.773	0.687
			0.24	0.45	0.18	7.76	J0106-1003	3.0	$5.018 \times 10^{-3}$	$6.455 \times 10^{-8}$	0.835	9.079
1.4	20.0	148.70	0.48	2916.81	0.0015	0.064	EMRI	0.05	$5.521 \times 10^{-10}$	$9.322 \times 10^{-13}$	0.808	und.
			0.45	0.59	0.45	19.92	WD0028-474	1.0	$3.868 \times 10^{-5}$	$3.106 \times 10^{-9}$	0.776	1.511
			0.43	0.52	0.47	21.30	WD0135-052	3.0	$2.660 \times 10^{-3}$	$6.344 \times 10^{-8}$	0.766	23.88
			0.42	0.51	0.45	20.25	WD1204-450	6.0	$4.148 \times 10^{-2}$	$4.377 \times 10^{-7}$	0.763	119.89
			0.41	0.47	0.47	21.48	WD1704-481 <sup>4</sup>	9.0	$2.135 \times 10^{-1}$	$1.375 \times 10^{-6}$	0.764	145.73

<sup>4</sup>Same chirp mass

## CEL: aftermath of binary white dwarf mergers



Isodensity curves of a CEL with polytropic index  $n = 2.95$ ,  $M_{\text{CEL}} = 1.2 M_{\odot}$ , and central density  $\rho_c = 1.2 \times 10^8 \text{ g cm}^{-3}$  rotating with angular velocity  $\Omega/\sqrt{\pi G \bar{\rho}_0} = 0.02$ . All the curves are *self-similar* to the ellipsoid with axes ratio  $a_2/a_1 = 0.68$  and  $a_3/a_1 = 0.77$ .



Density map of a section in the orbital plane (top panel) and in the polar plane (bottom panel) of a  $0.6 + 0.6 M_{\odot}$  DWD merger simulated with  $5 \times 10^4$  SPH particles. This snapshot is taken 9 orbital periods after mass transfer begins.

## Rates (Rodriguez, Rueda, Ruffini, Zuluaga, Iglesias-Blanco and Loren-Aguilar, JCAP 2023)

- ▶ Globular cluster → star with planetary companion → migration to the center and capture  
EMRI rate:  $0.02 - 0.5 \text{ yr}^{-1}$
- ▶ DWD, systems that will merger within Hubble time, rate  $0.0064 - 0.512 \text{ yr}^{-1}$
- ▶ CEL result of binary white mergers (no supernova)  $0.0056 - 0.45 \text{ yr}^{-1}$



## BNS merger (Juan Diego's Talk)

- ▶ BNS produced by a BdHN II, L. Becerra et al Universe 2023

	$m$ [ $M_{\odot}$ ]	$j$	$\Omega$ [ $s^{-1}$ ]	$R_{\text{eq}}$ [km]	$I$ [ $g \text{ cm}^2$ ]	$\Omega$ [ $s^{-1}$ ]	$R_{\text{eq}}$ [km]	$I$ [ $g \text{ cm}^2$ ]
			GM1 EOS			TM1 EOS		
$\nu$ NS	1.505	0.259	1114.6	14.03	$2.04 \times 10^{45}$	1077.1	14.47	$2.11 \times 10^{45}$
NS	1.404	-0.011	-52.14	14.01	$1.85 \times 10^{45}$	-56.6	14.49	$1.93 \times 10^{45}$

- ▶ Conservation of baryonic mass

$$M_b = m_{b,c} + m_{ej} + m_d, \quad M_b = m_{b,1} + m_{b,2}.$$

- ▶ The relation among its baryonic mass,  $m_{b,i}$ , gravitational mass,  $m_i$ , and angular momentum  $J_i$  is,

$$\frac{m_{b,i}}{M_{\odot}} \approx \frac{m_i}{M_{\odot}} + \frac{13}{200} \left( \frac{m_i}{M_{\odot}} \right)^2 \left( 1 - \frac{1}{130} j_i^{1.7} \right), \quad i = 1, 2, c,$$

- ▶ Conservation of angular momentum

$$J_{\text{merger}} = J_c + J_d + \Delta J,$$

## Remnant NS, maximal disk mass and no disk (Juan Diego's Talk)

- ▶ Conservation of mass-energy

$$E_{\text{GW}} + E_{\text{other}} = \Delta M c^2 = [M - (m_c + m_{\text{ej}} + m_d)]c^2, \quad (11)$$

- ▶ Limiting case with  $\Delta J = 0$ , which corresponds to the case with maximum disk mass,  $m_c = 2.697 M_{\odot}$ ,  $m_d = 0.073 M_{\odot}$ .

$$E_{\text{other}} = \Delta M c^2 = [M - (m_c + m_{\text{ej}} + m_d)]c^2 \approx (M - m_c - m_d)c^2 \quad (12)$$

$$\approx 0.139 M_{\odot} c^2 \approx 2.484 \times 10^{53} \text{ erg} \quad (13)$$

- ▶ Limiting case with  $m_d = 0$  which corresponds to the maximum angular momentum loss.  $\Delta J = 0.331 GM_{\odot}^2/c$ , and the maximum remnant's mass,  $m_c = 2.756 M_{\odot}$ ,  $E_{\text{GW}}^{\text{pm}} \approx 0.0079 M_{\odot} c^2 \approx 1.404 \times 10^{52} \text{ erg}$ .

$$\Delta M c^2 = [M - (m_c + m_{\text{ej}})]c^2 \approx (M - m_c)c^2 \quad (14)$$

$$\approx 0.153 M_{\odot} c^2 \approx 2.734 \times 10^{53} \text{ erg} \quad (15)$$

- ▶ Homopolar model
- ▶ Beyond pure gravitational quadrupole emission

$$\frac{\dot{\omega}_0}{\omega_0} = -\frac{\dot{P}}{P} = \frac{1}{g(\omega_0)} \left[ \dot{E}_{\text{GW}} - \frac{L}{1-\alpha} \right], \quad (16)$$

$$\frac{\dot{\alpha}}{\alpha} = -\frac{1}{g(\omega_0)} \left\{ \dot{E}_{\text{GW}} - \frac{L}{1-\alpha} \left[ 1 + \frac{g(\omega_0)}{\alpha I_1 \omega_0^2} \right] \right\}, \quad (17)$$

$$\frac{L}{1-\alpha} = 7.72 \times 10^{32} \left( \frac{\tilde{B}}{10^6 \text{ G}} \right)^2 \left( \frac{R_1}{10^9 \text{ cm}} \right)^6 \times \left( \frac{R_2}{10^9 \text{ cm}} \right)^2 \left( \frac{M_\odot}{M} \right)^{4/3} \left( \frac{100 \text{ s}}{P} \right)^{14/3} \text{ erg s}^{-1}, \quad (18)$$

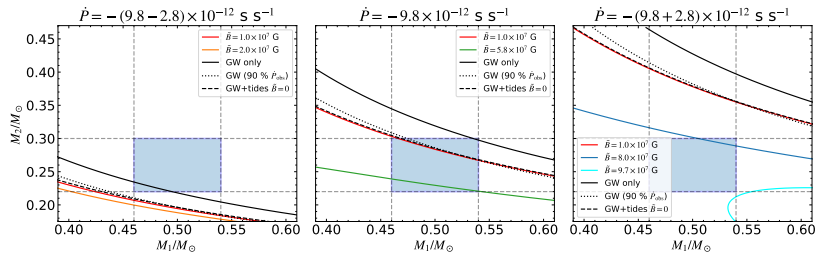


Figure 2: Constraints for SDSS J0651+2844.

Thank you

